J Mater Sci (2007) 42:3015–3023
DOI 10.1007/s10853-006-0521-x

Semi-empirical AM1 calculations on 6-memebered alumino-silicate rings model: implications for dissolution process of metakaoline in alkaline solutions

Zhang Yunsheng · Sun Wei

Received: 2 June 2005 / Accepted: 6 June 2006 / Published online: 22 February 2007

Abstract In order to investigate the dissolution process of metakaline in alkaline solutions, two 6-memebered rings models consisting of AlO_4 tetrahedron and SiO_4 tetrahedron, respectively are firstly proposed to represent the structure of metakaoline in this paper. Analysis of the dissolution mechanism of the two 6-memebered rings models in strongly solution reveals that the dissolution process of metakaoline is composed of ring breakage for releasing $HOTO_3^{\equiv}$ anion, formation of HO–$T(OM)_3$ by ion-pairing reaction between $HOTO_3^{\equiv}$ anion and M^+ cation, and further interaction between the remaining broken ring cluster and MOH solutions. A computational chemistry method: Semi-empirical AM1 calculation is then conducted on the two models to obtain the details of three steps involved in dissolution process. The calculated results showed that 6-member ring model consisting of AlO_4 tetrahedron is more reactive than 6-member ring model consisting of SiO_4 tetrahedron. Compared with local environment, strongly alkaline accelerated the dissolution of 6-member ring model consisting of SiO_4 tetrahedron. Na^+ has stronger ion-pairing interaction than K^+. The further reaction between the remaining broken ring cluster and strongly alkaline solution depended on the types of the remaining broken ring cluster and alkaline solution. The above results enhanced our understanding of dissolution mechanisms of metakaoline in highly alkaline solutions, which is especially important to geopolymerization reaction.

Z. Yunsheng (✉) · S. Wei
Department of Materials Science and Engineering,
Southeast University, Nanjing 210096, P.R. China
e-mail: zhangys279@163.com

Introduction

In recent years a novel type of high performance inorganic binder—Geopolymer is rapidly developed around the world. Compared to Portland cement, Geopolymer possesses low energy consumption, less CO_2 emission, high early strength, less shrinkage, low permeability, good fire and acid resistance and excellent durability [1]. These merits make Geopolymer exhibit promising potentials in the fields of civil, bridge, pavement, hydraulic, underground and militia engineering.

At present, research into formation process of Geopolymer has become a hot topic internationally. By far most of the researchers describe the formation process of Geopolymer by means of traditional hydration mechanism of Portland cement or alkali slag cement. Only a 3-steps process of dissolution–reorientation–polycondensation involved in geopolymerization reaction is proposed and discussed until now [1–5]. However, the 3-steps process almost takes place at the same time. Consequently, the dynamics of the 3 steps are inter-dependent, so that it is impossible to isolate the 3 steps in an experimental study, resulting in no better understanding of the details of each step.

The rate and extent of dissolution of alumino-silicate materials in alkali solutions directly determine

the types and amount of Geopolymeric products. Hence, it is essential to understand dissolution process involved in geopolymerization reaction in order to gain insight into the kinetics and mechanisms of geopolymerization. Considering the difficulty in isolating the 3 steps in experiment, molecular simulation is used in this paper to study the first step of geopolymerization reaction—dissolution process.

Some theoretical researches into dissolution mechanisms of silicates or alumino-silicate materials have been conducted in recent 20 years [6–29]. In most of these studies, researchers firstly postulated a molecular model representing the structure of the raw material, then analyzed the molecular model to obtain the kinetics and mechanisms of dissolution. The method is proved to be very feasible and effective to these problems that are very difficult to address through experimental studies.

Semi-empirical AM1 calculation has shown to be successful in predicting the molecular structure and physical properties of silicates or alumino-silicate materials. By far the important conclusions from these studies are that the major structures and energetics of silicates or alumino-silicates can be accounted for by short-range directional forces or covalent bonding in a traditional sense. As a result, finite molecular clusters can be used to simulate the local environment and provide significant insight into the atomic forces and bonding pictures of silicates or alumino-silicates. With the development of computational power of PC (personal computer), it is possible to calculate the bonding, breaking and formation processes, in particular, the reaction pathways and energetics involving silicates or alumino-silicates from the atomic point of view with AM1 calculation.

Kaolinite is one of the alumino-silicates without CaO. Its reactivity can be greatly improved after a suitable calcining regime. When the calcined kaolinite that is called metakaoline (MK) contacts with strongly alkaline solutions such as NaOH or KOH, a large amount of Si and Al clusters are dissolved to solutions. Rapid dissolution of MK in strongly alkaline solutions has made it become a key material of geopolymerization [30–51]. Therefore, it is very important to understand the kinetics and mechanisms of dissolution of MK in alkaline solutions. In this study, we firstly established a molecular model representing MK structure, and then study the dissolution behaviors of the model using semi-empirical AM1 calculation. The calculation can be used to understand the dissolution process of MK in alkaline solutions.

Molecular model representing MK structure

MK is a type of sheet molecular structure alumino-silicate materials. The sheet structure can be reproduced periodically by a few small molecular units [52]. Therefore, it is reasonable to assume that these small molecular units can be used to represent the structure of MK. Of course, the correct selection of small molecular units is a key to understand the kinetics and mechanisms of dissolution of MK.

Molecular structure of MK

Kaolinite will lose most of the structural H_2O after calcining. However, the sheet molecular structure of kaolinite can still be sustained in MK. By using MAS-NMR technique, it is found that the coordination environment of Si atom is not almost changed and still kept at 4-fold coordination, while great change will taken place for the coordination environment of Al atom varying from 6-fold to 4-fold coordination [53].

Based on the above analysis, we can imagine the molecular structured of MK, as shown in Fig. 1: MK is composed of two-sheet structure. One sheet is a SiO_4 tetrahedral layer similar to that of kaolinite, the other sheet is a greatly distorted AlO_4 tetrahedral layer transformed from $Al(OH)_6$ octahedral layer in kaolinite.

As can be seen from Fig. 1, there are mainly three types of reproduced units in MK: (1) SiO_4 and AlO_4 tetrahedral units; (2) Single 6-membered ring structure clusters consisting of SiO_4 and AlO_4 tetrahedron, respectively; (3) Double 6-membered ring structure clusters consisting of single 6-membered SiO_4 ring and AlO_4 ring clusters.

Herein it is worth noting that the metakaolin is actually X-ray amorphous, and contains a range of Al coordination [54]. The 6-membered rings of 4-coordinated Al are only an approximation to the actual structure in fact.

Molecular model representing MK structure

In order to accurately simulate the molecular structure of MK, and perform molecular calculations in PC, an important requisition is to choose a suitable molecular cluster to simulate the bulk solid of MK. Of primary concern is the size of the molecular cluster used in such calculations. This is because the computing time increases dramatically with an increase in the size of the cluster. On the one hand, the chosen molecular cluster should be sufficiently large to accurately mimic

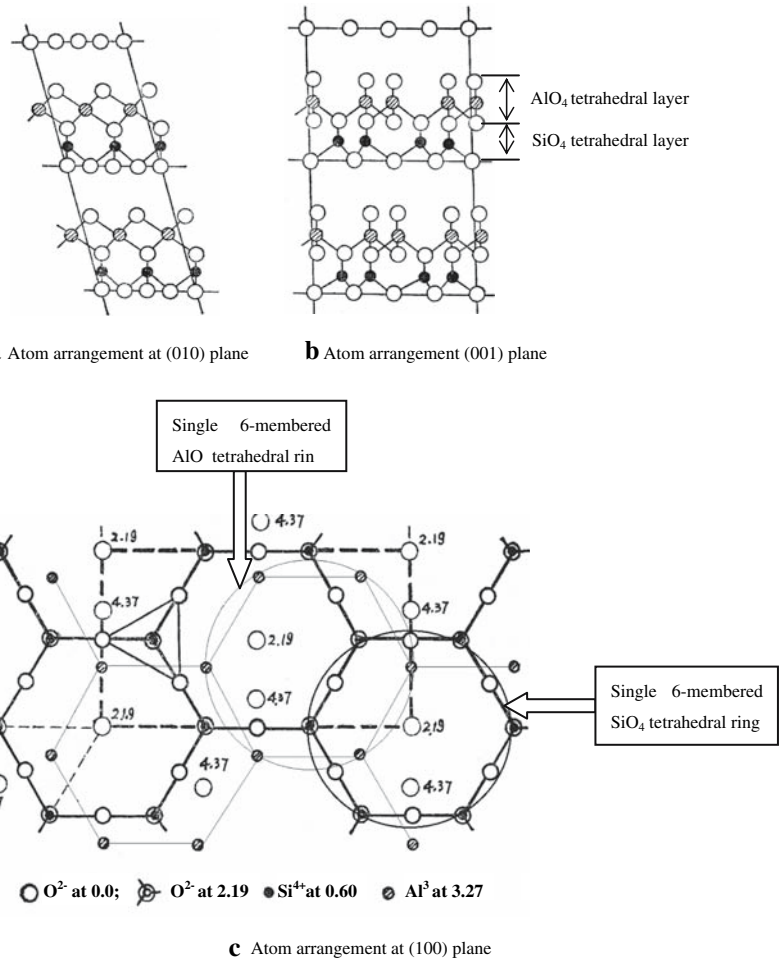

Fig. 1 Molecular structure of metakaoline (**a**) Atom arrangement at (010) plane. (**b**) Atom arrangement (001) plane. (**c**) Atom arrangement at (100) plane

the local environment of the molecular structure of MK. On the other hand, the molecular cluster should be sufficiently small to ensure computational feasibility.

As shown in Fig. 1, SiO_4 and AlO_4 tetrahedral units are the smallest reproduced molecular units of MK. Molecular calculations on these two units are very simple and easy. However, they do not embody the ring structural environment of MK, so that they are not considered as the molecular model representing the structure of MK. Both single 6-membered ring structure clusters and double 6-membered ring structure clusters can exhibit the ring structure environment. Considering that the computing time and memory requirements used in molecular calculations for double 6-membered ring structure clusters are almost 4–8 times greater than those for single 6-membered ring structure clusters caused by more atoms in double 6-membered ring structure clusters, single 6-membered SiO_4 and AlO_4 tetrahedron ring structure clusters are finally considered as the molecular models representing the structure of MK and discussed in detail in this study. In order to minimize the size of computing model and keep the balance of potential field, single 6-membered SiO_4 and AlO_4 tetrahedron ring structure clusters with all suspended bonds are terminated by OH groups. Figure 2 presents the 6-membered ring models representing the structure of MK. The bond length and angle of single 6-membered SiO_4 and AlO_4 tetrahedron ring models are also calculated using semi-empirical AM1 restricted Hatree-Fock calculations, as shown in Table 1.

Semi-empirical AM1 calculation of dissolution process of single 6-membered SiO_4 and AlO_4 tetrahedron ring models in local environment

Single 6-membered SiO_4 and AlO_4 tetrahedron ring models will produce bond breaking and releasing of $T(OH)_4$ clusters (T represents Si or Al) in local environment. The process can be modeled phenomenologically as follows:

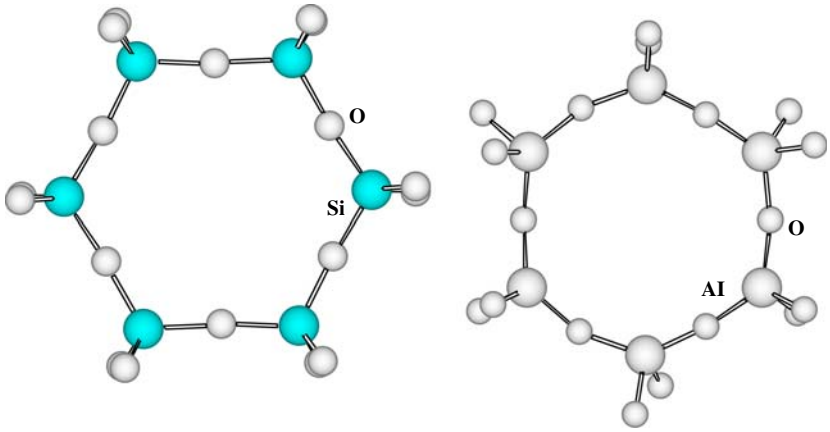

Fig. 2 Molecular models representing the structure of metakaoline. (**a**) 6-membered ring model of SiO_4 tetrahedron. (**b**) 6-membered ring model of AlO_4 tetrahedron

a 6-membered ring model of SiO_4 tetrahedron **b** 6-membered ring model of AlO_4 tetrahedron

$$(Si(OH)_2O)_6 + 2H_2O \Rightarrow (OH)_3Si{-}(Si(OH)_2O)_3 {-}Si(OH)_3 + HO{-}Si \equiv (OH)_3 \quad \Delta E1 \tag{1}$$

$$(Al^-(OH)_2O)_6 + 2H_2O \Rightarrow (OH)_3Al^-{-}(Al^-(OH)_2O)_3 {-}Al^-(OH)_3 + HO{-}Al^- \equiv (OH)_3 \quad \Delta E2 \tag{2}$$

Reaction energies $\Delta E1$, $\Delta E2$ can be obtained by using semi-empirical AM1 restricted Hatree-Fock calculations, shown in Table 2. The molecular models of the remaining broken ring structure model after releasing of $T(OH)_4$ from single 6-membered SiO_4 and AlO_4 tetrahedron ring models are presented in Fig. 3.

From Table 2, the reaction energy $\Delta E2$ caused by a releasing of $HO{-}Al^- \equiv (OH)_3$ is –1464.21 KJ/mol. This means that the dissolution process of single 6-membered AlO_4 tetrahedron ring is a strongly exothermic reaction. However, the opposite is true for 6-membered SiO_4 tetrahedron ring. This indicates that single 6-membered AlO_4 tetrahedron ring is more reactive than single 6-membered SiO_4 tetrahedron ring and more easily dissolved in local environment.

Semi-empirical AM1 study of dissolution process of single 6-membered $SiO_4$and AlO_4 tetrahedron ring models in strongly alkaline environment

As mentioned in the introduction, the dissolution of MK in strongly alkaline solutions is the important starting step in geopolymerization reaction. The objective of this study is to gain insight into the dissolution mechanism of MK in strongly alkaline solutions using semi-empirical AM1 calculations.

In strongly alkaline environment (pH > 14), more than 97.47% of $Si(OH)_4$ exists as $HOSiO_3^{\equiv}$ anion that will participate in ion-pairing reaction with alkali metal cation M^+ (M represents Na or K) to form $HOSi(OM)_3$ species [55]. However, no documented literature involved the state of $Al(OH)_4^-$ anion in alkaline solution can be found until now. Considering the similarity in chemical environment, it is reasonable to assume that $Al(OH)_4^-$ anion exists as $HOAl(OM)_3^-$ species in MOH solutions.

The dissolution process of sing 6-membered ring models can be divided into three steps in strongly alkaline solutions as shown from Eq. 3 to Eq. 10: (1) Ring breakage for releasing $HOSiO_3^{\equiv}$ or HO

Table 1 Bond length and angle in 6-membered ring models

Bond length (nm)		Bond angle (°)			
$Si–O_{nbr}$	$Si–O_{br}$	$O_{br}–Si–O_{br}$	$O_{br}–Si–O_{nbr}$	$O_{nbr}–Si–O_{nbr}$	$Si–O_{br}–Si$
a. Bond length and angle in 6-membered ring model of SiO_4 tetrahedron					
0.16931	0.1615	110.2564	106.8573	115.3440	159.8111
Bond length (nm)		Bond angle (°)			
$Al–O_{nbr}$	$Al–O_{br}$	$O_{br}–Al–O_{br}$	$O_{br}–Al–O_{nbr}$	$O_{nbr}–Al–O_{nbr}$	$Al–O_{br}–Al$
b. Bond length and angle in 6-membered ring model of AlO_4 tetrahedron					
0.17331	0.1755	98.0483	104.9156	131.2312	132.6833

Note: O_{br}—bridging oxygen, O_{nbr}—non-bridging oxygen

Table 2 Reaction energies of single 6-membered rings structure models in local environment

Molecular structure cluster	Formation heat (a.u)	Reaction heat (KJ/mol)	
		$\Delta E1$	$\Delta E2$
$(Si(OH)_2O)_6$	–1491.44763	77.43	–1464.21
$(Al^-(OH)_2O)_6$	–619.66576		
$(OH)_3Si$–$(Si(OH)_2O)_3$–$Si(OH)_3$	–1294.64502		
$(OH)_3Al^-$–$(Al^-(OH)_2O)_3$–$Al^-(OH)_3$	–776.45042		
$HO–Si \equiv (OH)_3$	–296.86927		
$HO–Al^- \equiv (OH)_3$	–310.33831		
H_2O	–59.25069		

AlO_3^{-IV} anion; (2) Formation of $HO–Si(OM)_3$ or $HO–Al^-(OM)_3$ species by ion-pairing reaction between $HOTO_3^{\equiv \text{ or } -IV}$ anion and M^+ cation; (3) Further interaction between the remaining broken ring cluster and MOH solutions.

$$(Si(OH)_2O)_6 + 3NaOH \Rightarrow (OH)_3Si{-}(Si(OH)_2O)_3 {-}Si(OH)_3 + HO{-}Si \equiv (ONa)_3 + H_2O \quad \Delta E3 \tag{3}$$

$$(Si(OH)_2O)_6 + 3KOH \Rightarrow (OH)_3Si{-}(Si(OH)_2O)_3 {-}Si(OH)_3 + HO{-}Si \equiv (OK)_3 + H_2O \quad \Delta E4 \tag{4}$$

$$(Si(OH)_2O)_6 + 4NaOH \Rightarrow (OH)_3Si{-}(Si(OH)_2O)_3 {-}Si(OH)_2{-}ONa + HO{-}Si \equiv (ONa)_3 + 2H_2O \quad \Delta E5 \tag{5}$$

$$(Si(OH)_2O)_6 + 4KOH \Rightarrow (OH)_3Si{-}(Si(OH)_2O)_3 {-}Si(OH)_2{-}OK{+}HO{-}Si \equiv (OK)_3 + 2H_2O \quad \Delta E6 \tag{6}$$

$$(Al^-(OH)_2O)_6 + 3NaOH \Rightarrow (OH)_3Al^-{-}(Al^-(OH)_2O)_3 {-}Al^-(OH)_3 + HO{-}Al^- \equiv (ONa)_3 + H_2O \quad \Delta E7 \tag{7}$$

$$(Al^-(OH)_2O)_6 + 3KOH \Rightarrow (OH)_3Al^-{-}(Al^-(OH)_2O)_3 {-}Al^-(OH)_3 + HO{-}Al^- \equiv (OK)_3 + H_2O \quad \Delta E8 \tag{8}$$

$$(Al^-(OH)_2O)_6 + 4NaOH \Rightarrow (OH)_3Al^-{-}(Al^-(OH)_2O)_3{-}Al^-(OH)_2{-}ONa + HO{-}Al^- \equiv (ONa)_3 + 2H_2O \Delta E9 \tag{9}$$

$$(Al^-(OH)_2O)_6 + 4KOH \Rightarrow (OH)_3Al^-{-}(Al^-(OH)_2O)_3 {-}Al^-(OH)_2{-}OK{+}HO{-}Al^- \equiv (OK)_3 + 2H_2O \Delta E10 \tag{10}$$

Equations (3) and (4), (7) and (8) represent the ring breakage as well as formation of $HOT(OM)_3$ species in strongly alkaline environment, which is similar to that in local environment (Eqs. 1, 2).

Equations (5) and (6), (9) and (10) include not only the ring breakage and formation of $HOT(OM)_3$ species, as in the case of Eqs. 3 and 4, 7 and 8, but also further interaction between the remaining broken ring cluster and MOH solutions. Therefore, the values of ($\Delta E5$–$\Delta E3$), ($\Delta E6$–$\Delta E4$), ($\Delta E9$–$\Delta E7$) and ($\Delta E10$–$\Delta E8$) actually represent the further interaction energies between MOH solutions and the remaining broken ring clusters.

Figures 4 and 5 show the molecular models of $HOT(OM)_3$ and the remaining broken ring clusters. Table 3 lists the reaction energies for Eqs. 3–10 using semi-empirical AM1 calculations. The bond length and angle of the remaining broken 6-membered SiO_4 and

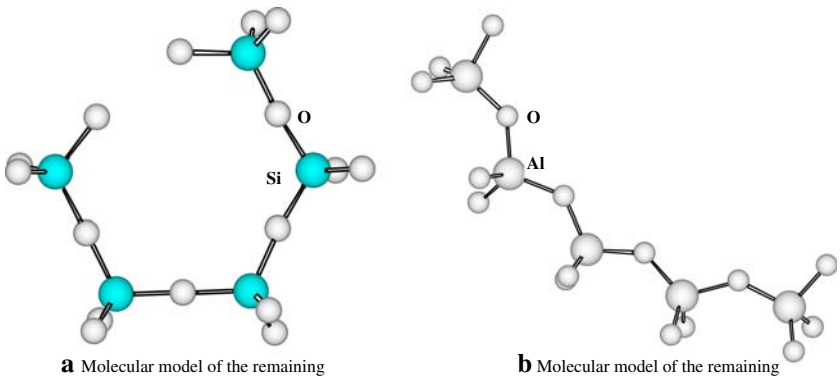

a Molecular model of the remaining broken ring after release of $Si(OH)_4$

b Molecular model of the remaining broken ring after release of $Al(OH)_4^-$

Fig. 3 Molecular models of the remaining broken ring after dissolution. (**a**) Molecular model of the remaining broken ring after release of $Si(OH)_4$. (**b**) Molecular model of the remaining broken ring after release of $Al(OH)_4^-$

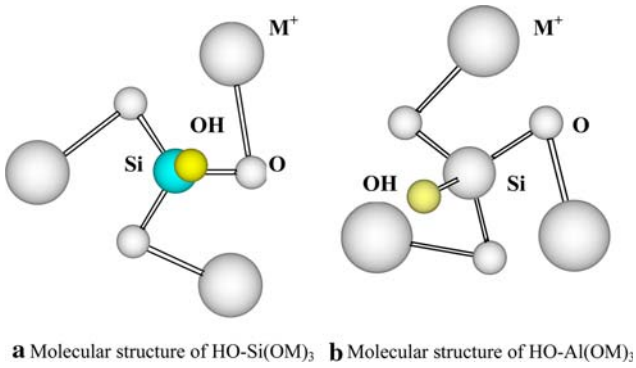

a Molecular structure of HO-Si(OM)$_3$ **b** Molecular structure of HO-Al(OM)$_3$

Fig. 4 Optimized molecular structure model of HO–T(OM)$_3$ (T represents Si or Al). (**a**) Molecular structure of HO–Si(OM)$_3$. (**b**) Molecular structure of HO–Al$^-$(OM)$_3$

AlO_4 tetrahedron ring models are also calculated using AM1 method in this paper. The changes in bond length and angle of the 6-membered rings models before and after dissolution in strongly alkaline solution are shown in Figs. 6 and 7.

As can be seen from Figs. 6 and 7, the bonds on boundary (Si–O_{br}) and bonds on ring (Si–O_{nbr}) are both stretched, while the angles on ring (O_{br}–Si–O_{br}) are reduced and the angles (Si–O_{br}–Si) are increased after the releasing of Si(OH)$_4$ cluster regarding single 6-membered SiO_4 tetrahedron ring model. This suggests that single 6-membered SiO_4 tetrahedron ring model contracts inwards after dissolution in strong alkaline environment, which can seen clearly in Fig. 5a, b.

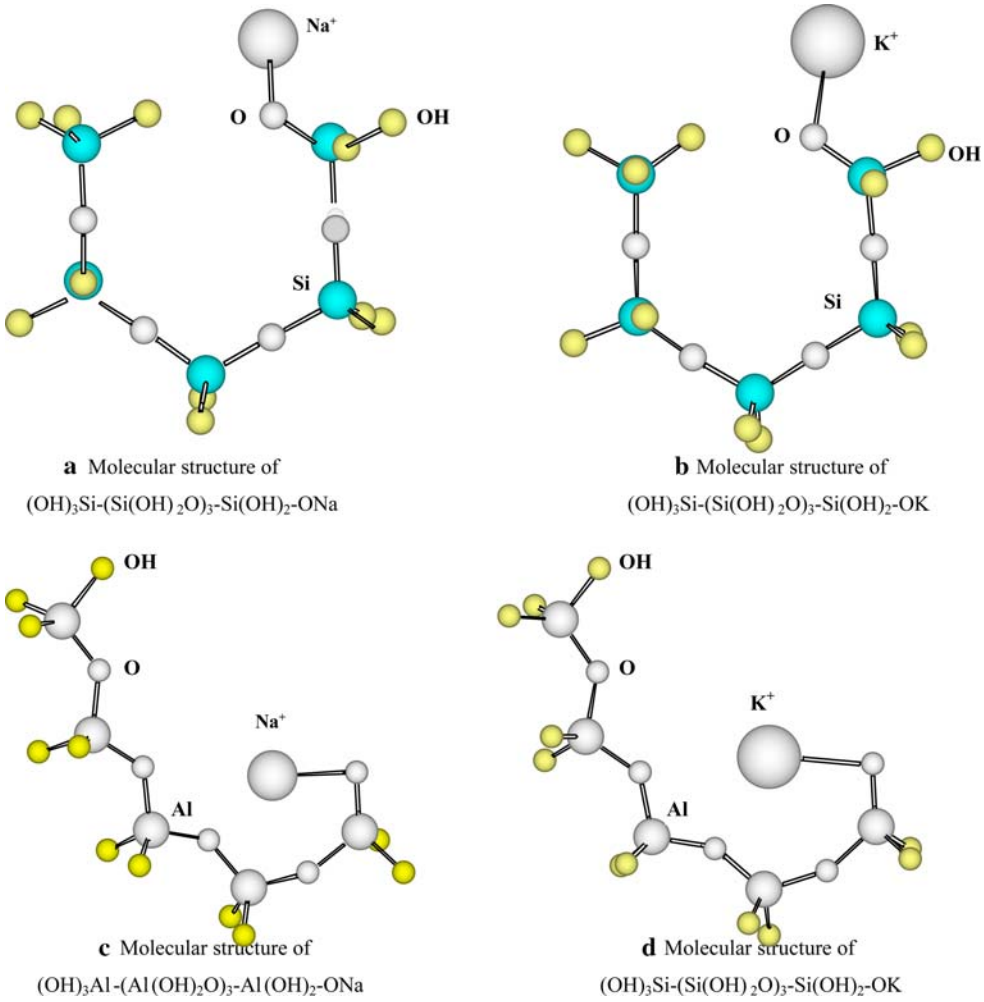

a Molecular structure of $(OH)_3Si$-$(Si(OH)_2O)_3$-$Si(OH)_2$-ONa

b Molecular structure of $(OH)_3Si$-$(Si(OH)_2O)_3$-$Si(OH)_2$-OK

c Molecular structure of $(OH)_3Al$-$(Al(OH)_2O)_3$-$Al(OH)_2$-ONa

d Molecular structure of $(OH)_3Si$-$(Si(OH)_2O)_3$-$Si(OH)_2$-OK

Fig. 5 Optimized molecular structure model of the remaining broken ring after dissolution of ion cluster (**a**) Molecular structure of $(OH)_3Si$–$(Si(OH)_2O)_3$–$Si(OH)_2$–ONa. (**b**) Molecular structure of $(OH)_3Si$–$(Si(OH)_2O)_3$–$Si(OH)_2$–OK. (**c**) Molecular structure of $(OH)_3Al^-$–$(Al^-(OH)_2O)_3$–$Al^-(OH)_2$–ONa. (**d**) Molecular structure of $(OH)_3Al^-$–$(Al^-(OH)_2O)_3$–$Al^-(OH)_2$–OK

Table 3 Reaction heat of single 6-membered rings models in strongly alkaline solution

Reaction heat (KJ/mol)							
$\Delta E3$	$\Delta E4$	$\Delta E5$	$\Delta E6$	$\Delta E7$	$\Delta E8$	$\Delta E9$	$\Delta E10$
–60.89	12.79	–227.43	–156.30	–1292.28	–1066.31	–1342.31	–1059.24

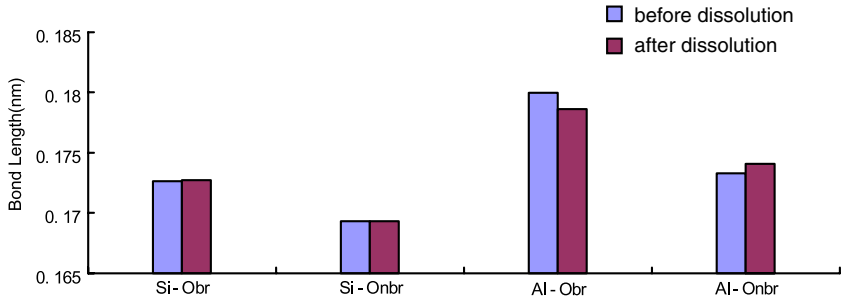

Fig. 6 Bond length change of single 6-membered rings models before and after dissolution in strongly alkaline solution

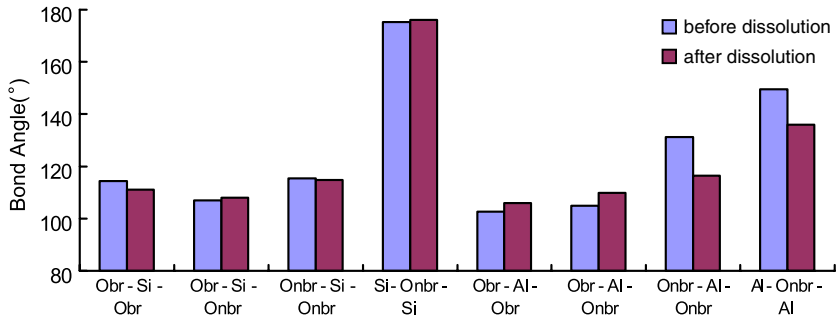

Fig. 7 Bond angle change of single 6-membered rings models before and after dissolution in strongly alkaline solution

For single 6-membered AlO_4 tetrahedron ring model, the reduction in the bonds on boundary (Al–O_{nbr}) and increase in the bond on ring (Al–O_{br}) are found after the releasing of $Al(OH)_4^-$ cluster. The angles on ring (O_{nbr}–Al–O_{br}) and (Al–O_{br}–Al) show a diminishing trend. This indicates that single 6-membered AlO_4 tetrahedron ring model expands outwards after dissolution in strong alkaline environment, which can be seen in Fig. 5c, d.

Based on the above analysis, we know that the single 6-membered ring models are readjusted after dissolution, resulting in some changes in bond length and angle.

From Table 3, the following observations could be obtained:

Alkaline environment significantly accelerate the dissolution process of single 6-membered ring models with much higher exothermal energies than local environment. For instance, dissolution energies in local environment ($\Delta E1$) is 77.43 KJ/mol that means it is endothermic reaction, while the corresponding value in NaOH ($\Delta E3$) is –60.89 KJ/mol that is exothermal reaction regarding single 6-membered SiO_4 tetrahedron ring model. In the case of KOH, dissolution energy ($\Delta E4$) shows less endothermic demand than local environment ($\Delta E1$).

It is also found that dissolution in NaOH exhibit higher heat releasing than that in KOH ($|\Delta E3| > -\Delta E4$, $|\Delta E5| > |\Delta E6|$, $|\Delta E7| > |\Delta E8|$, $|\Delta E9| > |\Delta E10|$), which means that NaOH favors the dissolution of MK. This result has been verified by our experimental results.

As can be seen from comparison of Eqs. 3 and 4, both of them include the releasing of $HOT_3^{\equiv}$ anion, and ion-pairing reaction between $HOT_3^{\equiv}$ anion and M^+ cation. The only difference between Eqs. 3 and 4 is that ion-pairing reaction in Eq. 3 is between $HOSiO_3^{\equiv}$ anion and Na^+ cation, while ion-pairing reaction in Eq. 4 is between $HOSiO_3^{\equiv}$ anion and K^+ cation. Therefore, $|\Delta E3| > -\Delta E4$ indicates that ion-pairing reaction between $HOSiO_3^{\equiv}$ anion and Na^+ cation is stronger than that between $HOSiO_3^{\equiv}$ anion and K^+ cation. Similarly, $|\Delta E3| < |\Delta E7|$, $-\Delta E4 < |\Delta E8|$ also show Na^+ has stronger ion-pairing capacity with $HOAl^-O_3^{\equiv}$ than K^+. By using MAS-NMR techniques, McCormick et al. [56–58] and Swaddle et al. [59] also found that alkali metal cation of smaller size favor ion-pairing reaction with silicate monomer species in alkaline solution, which is consistent with our calculated result.

$|\Delta E3| < |\Delta E7|$, $-\Delta E4 < |\Delta E8|$ show ion-pairing reaction between $HOAl^-O_3^{\equiv}$ and M^+ is stronger than that between $HOSiO_3^{\equiv}$ and M^+ in the same strongly alkaline solution.

The difference in reaction energy between $|\Delta E9|$ and $|\Delta E10|$ is 283.07 KJ/mol, which is the sum of 225.97 KJ/mol ($|\Delta E7| - |\Delta E8|$) and 57.10 KJ/mol ($|\Delta E9| - |\Delta E7|$)–($|\Delta E10| - |\Delta E8|$). In other words, 20.20% of the difference in the dissolution energy for T(Al) center dissolved in NaOH and KOH solution is contributed by stronger ion-pairing reaction, while 79.80% comes from further interaction between the remaining broken ring clusters and alkaline solution, as shown in Fig. 8. Similarly, the contribution on the difference in reaction energy caused by different type of alkaline solution (NaOH and KOH) for single 6-membered SiO_4 tetrahedral ring model is also calculated, as shown in Fig. 9.

For single 6-membered AlO_4 tetrahedral ring model, the further interaction energy between the remaining broken ring clusters and NaOH ($|E9| - |E7| = 50.03$ KJ/mol) is less than that between the remaining broken ring clusters and KOH ($|E10| - |E8| = -7.07$ KJ/mol). For single 6-membered SiO_4 tetrahedral ring model, the similar trends is also shown ($|E5| - |E3| = 166.54$ KJ/mol, $|E6| - |E4| = 143.51$ KJ/mol). This means that both Na^+ and K^+ can stabilize the remaining broken ring clusters with K^+ being slightly better.

Conclusion

Semi-empirical AM1 restricted Hatree-Fock calculations have been conducted on optimized geometries of 6-membered AlO_4 and SiO_4 tetrahedral ring models in order to better understand the dissolution process of Metakaoline in alkaline solutions. Based on the calculated results, the following conclusions can be drawn:

(1) Single 6-membered SiO_4 tetrahedron ring model shows a contracting inwards after dissolution in strong alkaline environment, while a moving outwards trend is found in single 6-membered AlO_4 tetrahedron ring model, which indicates that the structure of metakaoline will obviously distorte after the releasing of $T(OH)_4$.

(2) The dissolution mechanism of the 6-membered rings models in strongly alkaline solution is revealed to consist of ring breakage for releasing $HOTO_3^{\equiv}$ anion, formation of $HO\text{-}T(OM)_3$ by ion-pairing reaction between $HOTO_3^{\equiv}$ anion and M^+ cation, and further interaction between the remaining broken ring cluster and MOH solutions.

(3) 6-membered rings model of AlO_4 tetrahedron compared with 6-membered rings model of SiO_4 tetrahedron is more reactive and is easily broken to release $HOTO_3^{\equiv}$ anion in alkaline environment. Na^+ cation show stronger ring breakage and ion-pairing interaction than K^+ cation. The further reaction between the remaining broken ring cluster and strongly alkaline solution depended on the types of the remaining broken ring cluster and alkaline solution. KOH has slightly better in stabilizing the remaining broken ring clusters than NaOH. Therefore, NaOH solution compared with KOH is expected to give a higher dissolution extent of metakaoline and a faster formation of geopolymeric products.

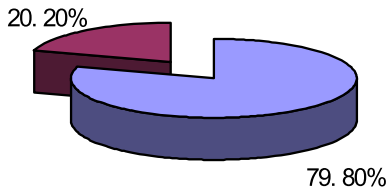

Fig. 8 Contribution of NaOH and KOH on the difference in dissolution heat of 6-membered rings of AlO_4

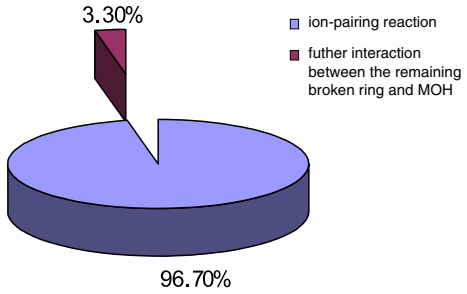

Fig. 9 Contribution of NaOH and KOH on the difference in dissolution heat of 6-membered rings of SiO_4

Acknowledgements Authors gratefully acknowledge the financial support from the china national natural science foundation (No. 50278018), Opening and flowing research project funded by Nanjing Hydraulic Research Institute (No. Yk90508), and the Jiangsu Province Natural Science project of No. BK2006555 and No. BK2005216.

References

1. Davidovits J (1991) J Thermal Anal 37(8):1633
2. van Jaarsveld JGS, van Deventer JSJ, Lorenzen L (1997) Minerals Eng 10(7):659
3. Granizo ML, Blanco-Varela MT, Palomo A (2000) J Mater Sci 35(24):6309
4. Provis JL, Duxson P, van Deventer JSJ, Lukey GC (2005a) Chem Eng Res Design 83(A7):853
5. Provis JL, Lukey GC, van Deventer JSJ (2005b) Chem Mater 17(12):3075
6. Xu H, van Deventer JSJ (2000) Comput Chem 24(3–4):391
7. Xu H, van Deventer JSJ, Roszak S, Leszczynski J (2004) Int J Quantum Chem 96(4):365

8. Lasaga AC, Gibbs GV (1990) Am J Sci 290(3):263
9. de Jong BHWS, Brown GE (1980) Geochim Cosmochim Acta 44(3):491
10. Lasaga AC, Gibbs GV (1990) Am J Sci 290(3):263
11. Kubicki JD, Sykes D (1995) Geochim Cosmochim Acta 59(23):4791
12. Pereira JCG, Catlow CRA, Price GD (1999b) J Phys Chem A 103(17):3268
13. Catlow CRA, George AR, Freeman CM (1996) Chem Comm (11):1311
14. Lasaga A (1984) J Geophy Res 89(B6):4009
15. Blum AE, Lasaga AC (1991) Geochim Cosmochim Acta 55(8):2193
16. Blum AE, Lasaga AC (1988) Nature 331(6155):431
17. Brady PV, Walther JV (1990) Chem Geol 82(3–4):253
18. Casey WH, Sposito G (1992) Geochim Cosmochim Acta 56(10):3825
19. Oelkers EH, Schott J, Devidal JL (1994) Geochim Cosmochim Acta 58(9):2011
20. Faimon J (1996) Geochim Cosmochim Acta 60(15):2901
21. Walther JV (1996) Am J Sci 296(7):693
22. Xiao Y, Lasaga AC (1996) Geochim Cosmochim Acta 60(13):2283
23. Bauer A, Velde B, Berger G (1998) Appl Geochem 13(5):619
24. Ejaz T, Jones AG, Graham P (1999) J Chem Eng Data 44(3):574
25. Huertas FJ, Chou L, Wollast R (1999) Geochim Cosmochim Acta 63(19–20):3261
26. Hamilton JP, Brantley SL, Pantano CG, Criscenti LJ, Kubicki JD (2001) Geochim Cosmochim Acta 65(21):3683
27. Oelkers EH (2001) Geochim Cosmochim Acta 65(21):3703
28. Köhler SJ, Dufaud F, Oelkers EH (2003) Geochim Cosmochim Acta 67(19):3583
29. Tsomaia N, Brantley SL, Hamilton JP, Pantano CG, Mueller KT (2003) Am Mineral 88(1):54
30. Davidovits J (1988) In: Proceedings of the First European Conference on Soft Mineralogy, France: Compiegne, pp 25–48
31. Davidovits J, Comrie DC, Paterson JH, Ritcey DJ (1990) Design Construct 12(7):30
32. Davidovits J, Davidovits M (1991) In: 36th Annual SAMPE Symposium. California, Covina: Society for the Advancement of Material and Process Engineering, pp 1939–1949
33. Davidovits J (1993a) Ceram Transac 37:165
34. Davidovits J (1993b) In: Emerging technologies on cement and concrete in the global environment. Symposium. Chicago IL SKOKIE, IL, PCA, USA, p 21
35. Davidovits J (1994a) Concrete Int 16(12):53
36. Davidovits J (1994b) J Mater Edu 16(2&3):91
37. Davidovits J (1994c) In: Mehta PK (ed) Concrete technology, past, present, and future. American Concrete Institute SP-144, Detroit, pp 383–397
38. Davidovits J (1994d) In: Proceedings of the First International conference on Alkali Cements and Concretes, Scientific, Ukraine, KIEV, pp 131–149
39. Lyon RE, Foden A, Balaguru PN, Davidovits M, Davidovits J (1997) J Fire Mater 21:67
40. Lyon RE, Sorathia U, Balaguru PN, Foden A, Davidovits J, Davidovits M (1996) In: Proceedings of the first International Conference on Fiber Composites in Infrastructure (ICCI'96). Dept. Civil Eng., University of Arizona, USA, Tucson Arizona, pp 972–981
41. Davidovits J (1999) In: Proceedings of Geopolymere '99. Institute Geopolymer, France, Saint-Quentin, pp 9–40
42. Van Jaarsveld JGS, Van Deventer JSJ (1999) Cement Concrete Res 29(8):1189
43. Van Jaarsveld JGS, Van Deventer JSJ, Lorenzen L (1998) Metall Mater Transac B 29B:283
44. Van Jaarsveld JGS, Van Deventer JSJ, Schwartzman A (1999) Minerals Eng 12(1):75
45. Hua X, Van Deventer JSJ (2000) Int J Miner Process 59:247
46. Phair JW, Van Deventer JSJ (2001) Mineral Eng 14(3):289
47. Palomo A, Blanco Varela MT, Granizo ML et al (1999) Cement Concrete Res 29(7):997
48. Alonso S, Palomo A (2000) Cement Concrete Res 31(1):25
49. Alonso S, Palomo A (2001) Mater Lett 56(3):127
50. Palomo A, Grutzeck MW, Blanco MT (1999) Cement Concrete Res 29(8):1323
51. Barbosa VFF, Mackenzie KJD, Thaumaturgo C (2000) Int J Inorg Mater 2(4):309
52. Pawl F (1989) Structural chemistry of silicates: structure, bonding formation and classification. Xi Yaozhong trans., Beijing, China: the China Binding and industrial Press
53. Ding Z, Zhang D, Wang X (1997) Bull Chinese Ceram Soc 4:57
54. Rocha J, Klinowski J (1990) Angewandte Chemie – Int Ed, English 29(5):553
55. Babushkin VT, Matveyev GM, Mchedlov-Petrossyan OP (1985) Thermodynamics of silicates. Springer-Verlag, Berlin, pp 276–281
56. McComick AV, Bell AT, Raddke CJ (1989) J Phys Chem 93(5):1733
57. McComick AV, Bell AT, Raddke CJ (1989) J Phys Chem 93(5):1737
58. McComick AV, Bell AT, Raddke CJ (1989) J Phys Chem 93(5):1747
59. Swaddle TW, Salerno J, Tregloan PA (1994) Chem Soc Rev 23:319